

Numerical analysis of internal flow and mixing performance in polymer extruder II: twin screw element

Naksoo Kim*, Hongbum Kim and Jaewook Lee¹

Dept. of Mechanical Engineering, Sogang University,

¹Dept. of Chemical and Biomolecular Engineering, Sogang University, 1, Sinsu-dong, Mapo-gu, Seoul 121-742, Korea

(Received June 6, 2006; final revision received August 28, 2006)

Abstract

We analyzed the non-Newtonian and non-isothermal flow with Carreau-Yasuda viscosity model in co-rotating and counter-rotating twin screw extruder systems. The mixing performances with respect to the screw speed, the screw pitch, and the rotating direction have been investigated. The dynamics of mixing was studied numerically by tracking the motions of particles. The extent of mixing was characterized in terms of the deformation rate, the residence time distribution, and the average strain. The results showed that the high screw speed decreases the residence time but increases the deformation rate. Small screw pitch increases the residence time. It is concluded that the high screw speed increases the dispersive mixing performance, while the small screw pitch increases the distributive mixing performance. Co-rotating screw extruder has the better conveying performance and the distributive mixing performance than counter-rotating screw extruder with the same screw speed and pitch. Co-rotating screw extruder developed faster transport velocity and it is advantageous the flow characteristics to the mixing that transfers polymer melt from one barrel to the other barrel.

Keywords : nano-composites, polymer extrusion process, co-rotating twin screw extruder, counter-rotating twin screw extruder, mixing performance, particle tracking, residence time distribution

1. Introduction

Production through twin screw extruder is an important polymer extrusion process that is used for high molecular material like high viscous polymer melt. Twin screw extruder is divided into intermeshing screw extruder and non-intermeshing screw extruder according to the center-line distance. Also according to the rotation direction and the organization of screws, the twin screw extruder is classified into the co-rotating type in which two screws rotate in the same directions and the counter-rotating type in which two screws rotate in the opposite directions. Intermeshing co-rotating and counter-rotating screw extruders that are widely used for industry are employed differently based on purpose.

Even though it is necessary to figure out the flow characteristics and to collect available data for actual work, most numerical analyses about extrusion process have been done with excessive simplification of shape and many assumptions in most studies due to the difficulty of complicated shape modeling of twin screw extruders. Modeling with approximate shape is proper for basic tendency of

flow, but it has the limit to figure out the flow in a screw extruder accurately.

Kajiwara *et al.* (1996) studied the flow in co-rotating and counter-rotating screw extruders consisting of thin flight screw and open c-shaped channel. He analyzed the difference of flow according to the rotation direction and investigated the trace of massless particles in a screw extruder based on the calculated flow field. Also, by comparing the residence time distribution of polymer particles traced, he estimated the mixing performance of each screw extruder. Jaluria *et al.* (1996) performed a numerical analysis about a complicated twin screw extruder using a simplified shape model, and Cheng and Zloczower (1998) performed the non-isothermal flow simulation in a co-rotating screw extruder with the 3-D FEM commercial code, FIDAP. Both Bravo and Hrymak (2000) and Ishikawa *et al.* (2000) performed numerical analyses about extruders with co-rotating kneading elements.

Yoshinaga *et al.* (2000) simulated the flow in an extruder with co-rotating kneading elements using FEM and estimated the mixing performance of extruder with the marker tracking method. Shearer and Tzoganakis (2000) obtained the mixing performance by experiments using a microscopic probe in analyzing the interfacial reaction between polymer tracers in a twin screw extruder.

*Corresponding author: nskim@sogang.ac.kr
© 2006 by The Korean Society of Rheology

Ishikawa and Amano (2002) compared the mixing performance with respect to various shapes of screws and Bakalis and Karwe (2002) compared the velocity and the mass flux distribution in the nip and the translation regions. Bravo *et al.* (2004) analyzed the mixing performance of twin screw extruder based on the velocity field found in his previous study. Ye *et al.* (2005) performed a research about extrusion process of polymer melt by FEM with a 4-step fractional method. Linjie *et al.* (2005) analyzed polymerization reaction degree with respect to operation conditions using a commercial fluid flow program, FLUENT.

In this study, we model the intermeshing co-rotating and counter-rotating screw elements widely used for industry without approximating geometry. The models are simulated to obtain the velocity and the temperature fields for the investigation of the flow characteristics in the screw element. Based on the computation results, we try to figure out the effects of process conditions and analyze the mixing performance with respect to the rotation speed, the pitch length, and the rotation direction of screws. The flow in a screw extruder is non-steady state since the flow channel varies with time due to the rotation of the screw element in a barrel. As the flow in the screw extruder that is a dynamic boundary problem, we tried to increase the accuracy of analysis results by regarding the problem as a 3-D, unsteady states, and non-isothermal flow.

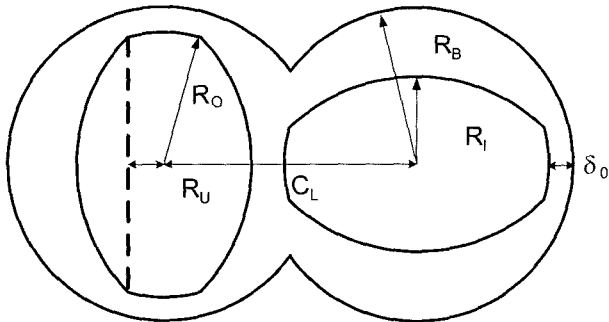


Fig. 1. Cross section of twin screw extruder.

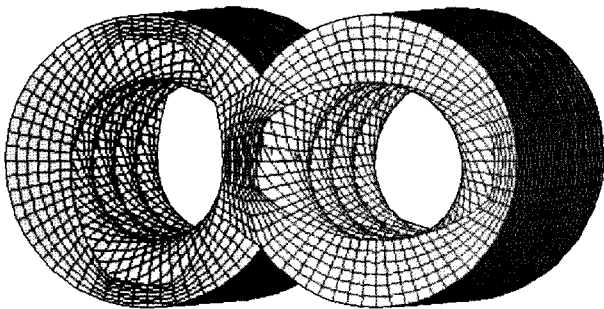


Fig. 2. Twin screw extruder model.

2. Geometry and process parameters

2.1. Geometry of twin screw extruder

Fig. 1 shows the cross section shape of barrel and screws and Fig. 2 illustrates the analysis domain of a twin screw extruder. Dimensions of the cross section are listed in Table 1. The barrel length for modeling is taken to 40 mm considering the computation efficiency. It is to reduce the computation time. Fig. 3 shows the arrangements of screws used for the numerical simulation.

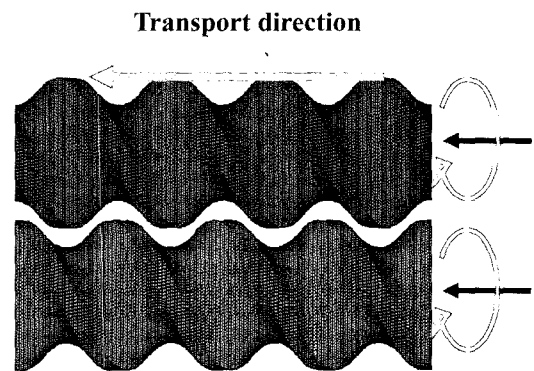
2.2. Assumptions and boundary conditions

The same assumptions and boundary conditions used in the previous study of the authors (Kim *et al.*, 2006) are applied for the flow analysis of twin screw element. Assumptions are summarized as follows:

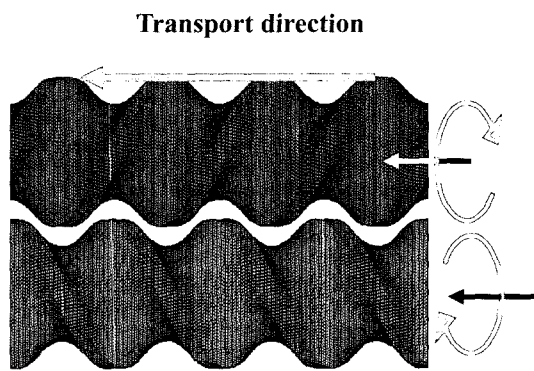
- (1) The flow regime in screw extruder is laminar.
- (2) The polymer melt is an incompressible fluid.

Table 1. Dimensions of twin screw extruder

C_L	R_B	R_O	R_I	R_U	δ_0
21 mm	13 mm	11 mm	7 mm	3 mm	2 mm



(a) co-rotating twin screw



(b) counter-rotating twin screw

Fig. 3. Arrangement of screws.

- (3) The viscosity is modeled to a function of temperature and shear rate.
- (4) Heat is generated due to the viscous dissipation of polymer melt.
- (5) Thermal condition between the screw surface and the polymer melt is adiabatic.
- (6) The no-slip condition is imposed onto the solid boundary.
- (7) Density and specific heat are constant.
- (8) The barrel is fully filled with polymer melt.
- (9) The steady state flow of polymer melt is attained after the screw rotates enough revolutions. During each time step, the screw rotates by a given angle.
- (10) Pressures at inlet and outlet are set to be zero.

2.3. Modeling procedure of analysis domain

The modeling procedure is the same as used in the single screw element in the previous study except the number of screws and the direction of rotating angles. It is summarized as follows:

- (1) Model the screw shape using I-DEAS as shown in Fig. 4(a) and transform the modeled screw surface to the shell mesh.
- (2) Model the barrel cavity mesh in STAR-CD as shown in Fig. 4(b).
- (3) Overlap the screw shell mesh and the fluid mesh in barrel cavity as shown in Fig. 4(c)
- (4) Rotate the screw shell mesh according to the screw rotation speed and project the fluid mesh to the rotated screw shell mesh. After subtracting the screw mesh from the barrel cavity at each rotating angle, the completed cavities are ready for the calculation, as shown in Fig. 4(d). As a result, the same number of barrel cavities is modeled as the number of specified rotating angles.

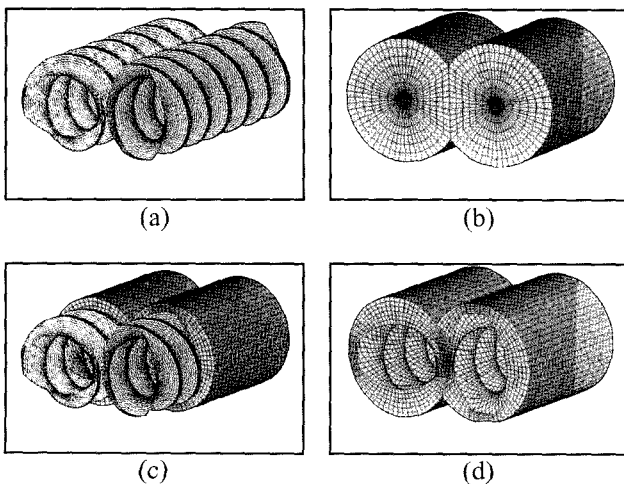


Fig. 4. Modeling procedure of analysis domain.

3. Viscous model and mixing index

3.1. Viscous model

The governing equations used in this numerical analysis are explained in Kim *et al.* (2006). The viscous model used in the calculation is Carreau-Yasuda model. This model as a function of shear rate and temperature is expressed by the equation (1). It is transformed to user subroutine to be used in STAR-CD.

$$\mu = \mu_0 \alpha [1 + (\lambda \dot{\gamma})]^{(n-1)} \quad (1)$$

In equation (1), α is a temperature shift factor, $\dot{\gamma}$, the shear rate expressed as follows:

$$\alpha = \exp\left[\beta\left(\frac{1}{T} - \frac{1}{T_{ref}}\right)\right] \quad \text{and} \quad \dot{\gamma} = \sqrt{\frac{1}{2}(s_{ij}s_{ij} - s_{ii}s_{jj})}$$

where T_{ref} is a reference temperature, β , the temperature sensitivity of μ , λ , the time constant, μ_0 , the zero shear viscosity, n , the power-law index. The values and the converging scheme with the cut-off method used in the computation are the same as in Kim *et al.* (2006).

3.2. Mixing index

The dispersive mixing index used in this study is a magnitude of deformation rate expressed by the equation (2). On the other hand, the distributive mixing index used in this study is the residence time distribution and the magnitude of strain.

$$|\dot{\gamma}(t)| = \left[2\left(\frac{\partial u}{\partial x}\right)^2 + 2\left(\frac{\partial v}{\partial y}\right)^2 + 2\left(\frac{\partial w}{\partial z}\right)^2 + \left(\frac{\partial v}{\partial x} + \frac{\partial u}{\partial y}\right)^2 + \left(\frac{\partial w}{\partial y} + \frac{\partial v}{\partial z}\right)^2 + \left(\frac{\partial u}{\partial z} + \frac{\partial w}{\partial x}\right)^2 \right]^{\frac{1}{2}} \quad (2)$$

The residence time distribution as defined in Kim *et al.* (2006) is as follows:

$$F(t) = C_{out}(t)/C_{\infty} \quad (3)$$

where $C_{out}(t)$ is the number of particles that arrive at outlet according to time and C_{∞} is the total number of tracking particles. Another index for the distributive mixing performance, the magnitude of strain is expressed by equation (4).

$$\gamma(t) = \int_0^t \dot{\gamma}(t) dt \quad (4)$$

4. Results and discussion

4.1. Flow characteristics in twin screw extruder

The flow characteristics of polymer melt are investigated in the co-rotating screws. All the results presented here are obtained in the middle cross section of the domain in the axial direction. The distribution of x -directional velocity component u is high near the screw surfaces as shown in

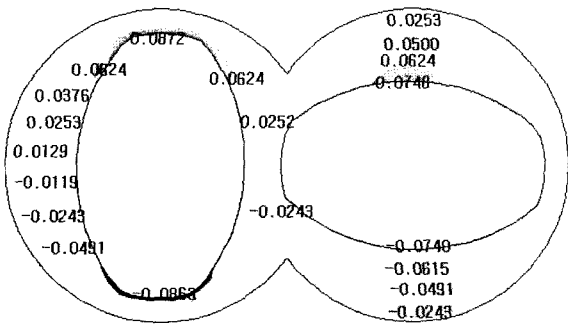


Fig. 5. Velocity [m/s] component u distribution in x - y plane [Pitch = 15 mm, rpm = 90].

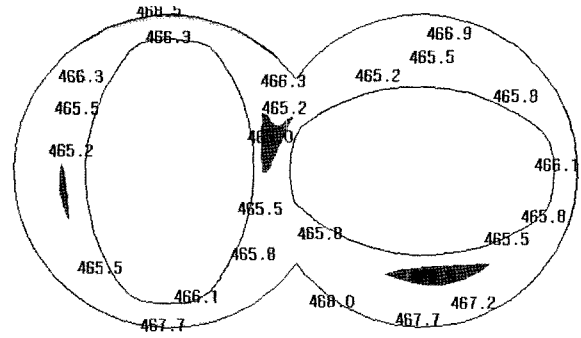


Fig. 8. Temperature [K] distribution in x - y plane [Pitch = 30 mm, rpm = 90].

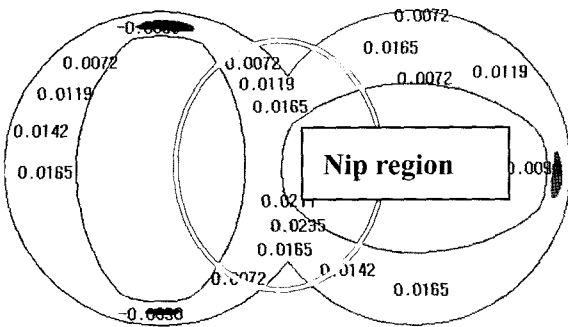


Fig. 6. Velocity [m/s] component w distribution in x - y plane [Pitch = 15 mm, rpm = 90].

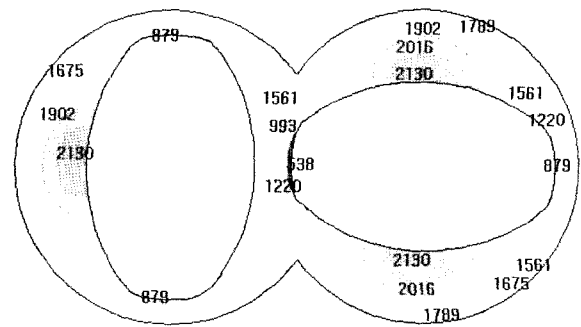


Fig. 9. Viscosity [Pa-s] distribution in x - y plane [Pitch = 30 mm, rpm = 90].

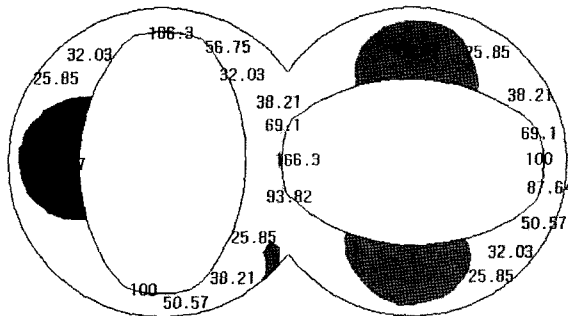


Fig. 7. Deformation rate [1/s] distribution in x - y plane [Pitch = 30 mm, rpm = 90].

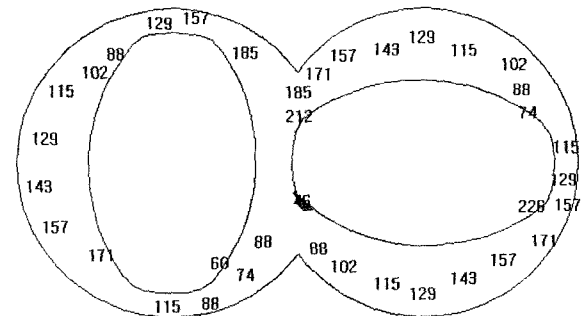


Fig. 10. Pressure [kPa] distribution in x - y plane [Pitch = 30 mm, rpm = 90].

Fig. 5. Similar tendency in the distribution of y -directional velocity component v is obtained. The distribution of z -directional velocity component w is different from u and v . It is higher in the intermeshing region (the nip region) than in the translation region where two screws don't cross over as shown in Fig. 6. This is resulted from the additive displacement effect due to the phase difference of two screws in the nip region.

The deformation rates are high in the gap and the nip regions as shown in Fig. 7. This characteristic has two meanings. One is that the effect of dispersive mixing is high in the gap and the nip and the other is that the temperature

is high where the deformation rate is high, due to the heat generation by the viscous dissipation as shown in Fig. 8.

Fig. 9 shows the viscosity distribution in the cross section. Viscosity as a function of temperature and deformation rate is inversely proportional to temperature and deformation rate. Therefore, the viscosity is relatively low in the nip and gap regions where the deformation rate is higher than that in the surrounding region. This is generally resulted from the typical shear thinning characteristic of polymer melt.

Fig. 10 shows the pressure distribution in the cross section. It should be noted that the pressure distribution is

higher in front of the gap region in the rotational direction than that in the back of the gap region. This is resulted from the reduction of available space for the flow of polymer melt. Therefore, we can expect that the pressure will be higher as the gap region is getting smaller.

4.2. Flow and mixing characteristic with respect to parameter

The velocity component, w , influences the mass flux distribution. As the screw rotation speed and the pitch length increase, the mass flux at outlet increases as shown in Fig. 11 because of the increase of the velocity component w . Fig. 12 shows the residence time distribution of polymer

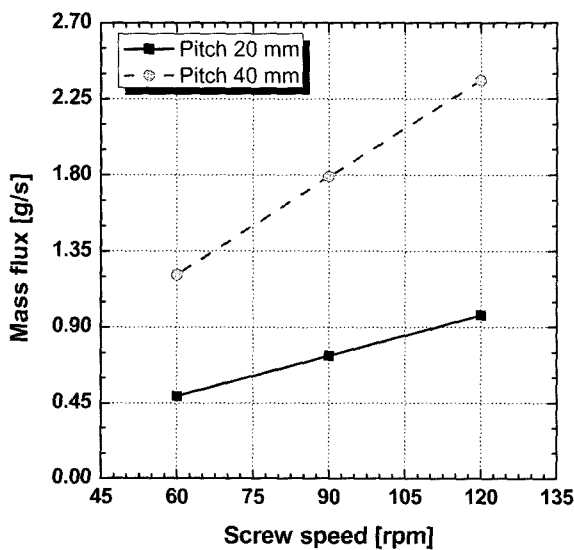


Fig. 11. Total mass flux with respect to screw speed and screw pitch length.

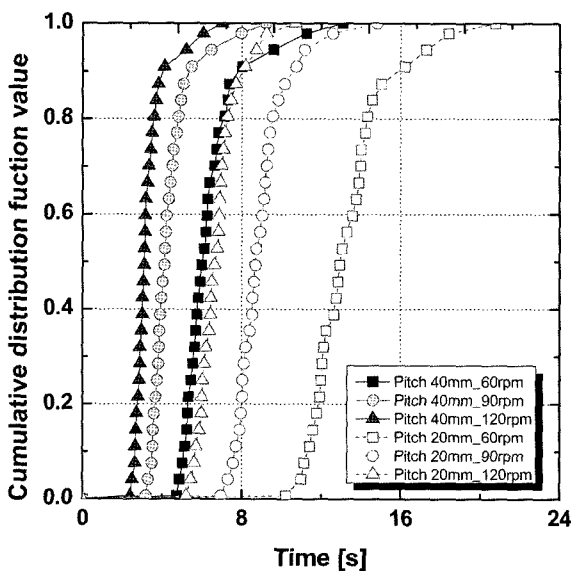


Fig. 12. Residence time obtained from the numerical tracers.

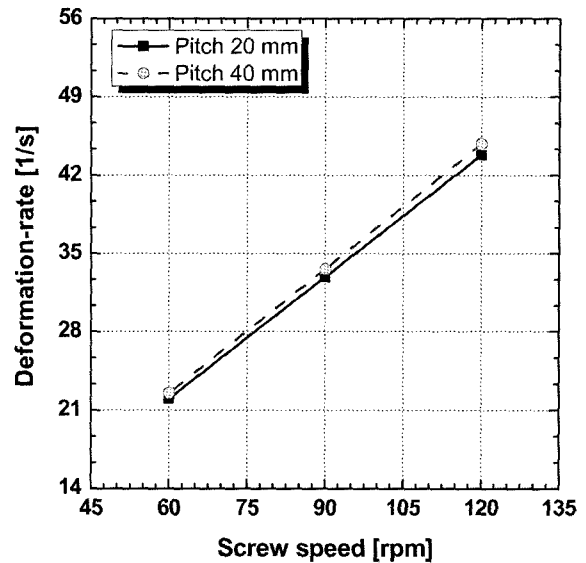


Fig. 13. Deformation-rate with respect to screw speed and screw pitch length.

melt. In the figure, as the screw rotation speed reduces and the pitch is smaller, the shift of curve to the right means the increase of residence time. Being gentle of the curve slope means the rise of macro-mixing performance. The initial location of particles and number of particles used in this study are the same as in Kim *et al.* (2006).

As shown in Fig. 13, the deformation rate increases as the screw rotation speed and the pitch length increase. But the difference of deformation rate with respect to the screw pitch length is negligible. So, the dispersive mixing performance will increase as the screw rotation speed rises, while the influence of screw pitch length on the dispersive mixing performance is little. On the other hand, the degree of elongation and shear rate that are components of deformation rate is different with respect to screw pitch length. In other words, elongation rate is higher at long screw pitch length while shear rate is higher at short screw pitch length as shown in the Fig. 14.

Total strain that is used as a distributive mixing index is shown in Fig. 15. It is obtained by integrating the calculated deformation rate with respect to the residual time at each time increment. Generally, the strain is proportional to the residence time and the deformation rate. So, when the screw pitch length is smaller, the strain increases due to the increase of residence time and the distributive mixing performance increases. On the other hand, the rise of screw rotation speed increases the deformation rate but reduces the residence time. The decrease of residence time offsets the effect that raises the strain due to the increase of deformation rate. The generalization of strain tendency according to the rise of screw speed is not straight forward. Even though the screw speed increases, the increase of the deformation rate and the decrease of the residence time will be

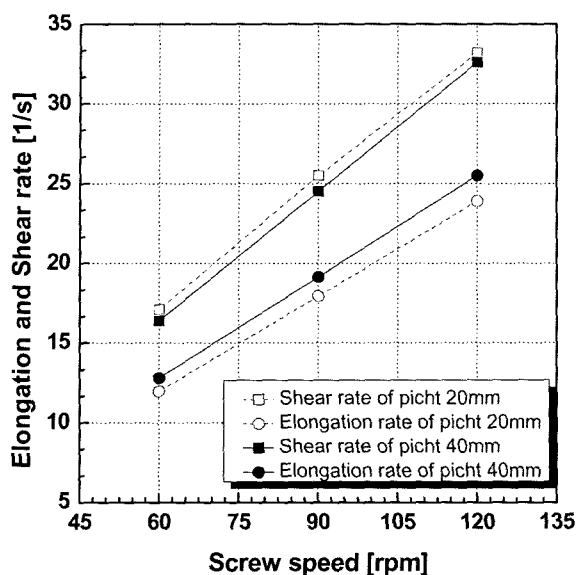


Fig. 14. Elongation and shear rate with respect to screw speed and screw pitch length.

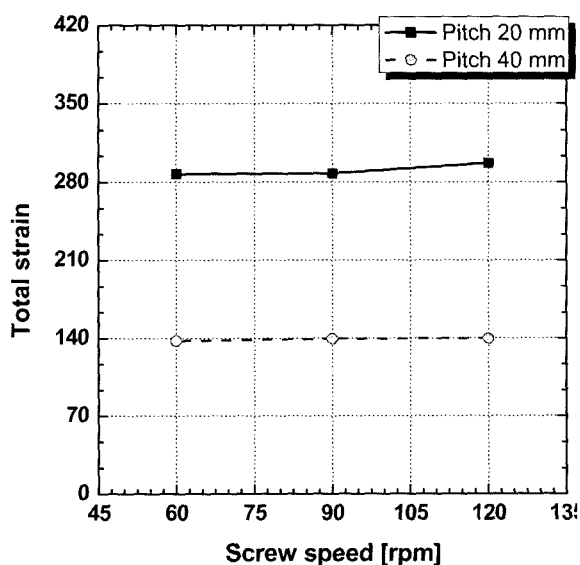


Fig. 15. Strain with respect to screw speed and screw pitch.

dependent to the specific screw shape. It is necessary to find the optimal screw speed that gives the maximum mixing performance according to a specific screw shape.

4.3. Flow characteristic of counter-rotating screw extruder

The distribution of velocity field, viscosity, pressure, and deformation rate and the principal of distribution in the counter-rotating screw extruder are similar to those in the co-rotating screw extruder explained in section 4.1. But there are many differences according to the screw rotating direction. Fig. 16 shows the velocity vectors in the cross

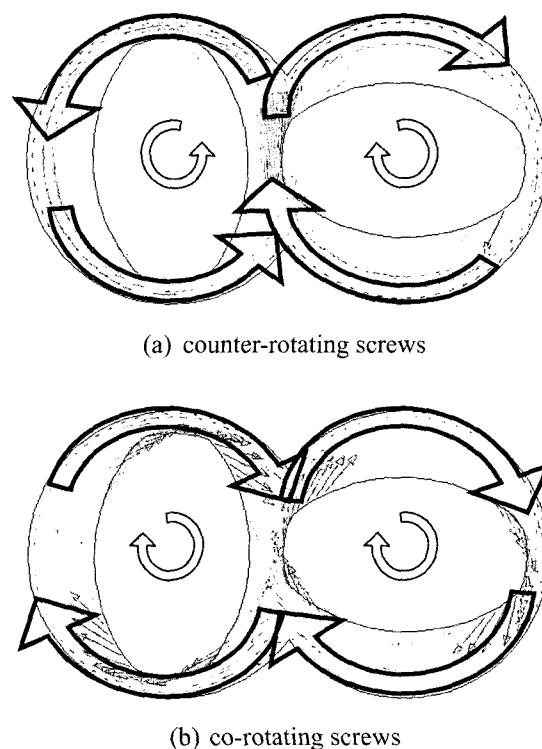


Fig. 16. Velocity vector in the cross section.

section of screw extruder at each screw rotating direction. The difference of flow pattern is shown in the nip region. The velocity components u , v are faster in the nip region of the counter-rotating screw extruder. The quantity of polymer melt entering the nip region is large since the screw velocities in the nip region are in the same direction and the polymer melt from both side translation regions accelerates to the same direction in the nip region.

The pressure at the nip region in the counter-rotating screw extruder is higher than that of the co-rotating screw extruder with the same pitch (30 mm) and screw speed (90 rpm) as indicated by circles in Fig. 17. Besides, as the screw speed increases and the distance between screws in the nip region is smaller, the pressure at the nip region is higher. The reason is that the quantity of polymer melt passing through the nip region increases and available space for the flow of polymer melt decreases. The high pressure in the nip region may cause deflection of screw shafts. Therefore it is more difficult to operate counter-rotating screw extruder with high speed than co-rotating screw extruder's case.

In case of the co-rotating screw extruder as shown in Fig. 16(b), the velocity components u , v in the nip region are smaller. Since the polymer melts in both side translation regions comes from the reverse directions each other and meets together in the nip region. Meanwhile, the co-rotating screw extruder conveys the polymer melt with the flow pattern shown in Fig. 5. The flow pattern transfers polymer

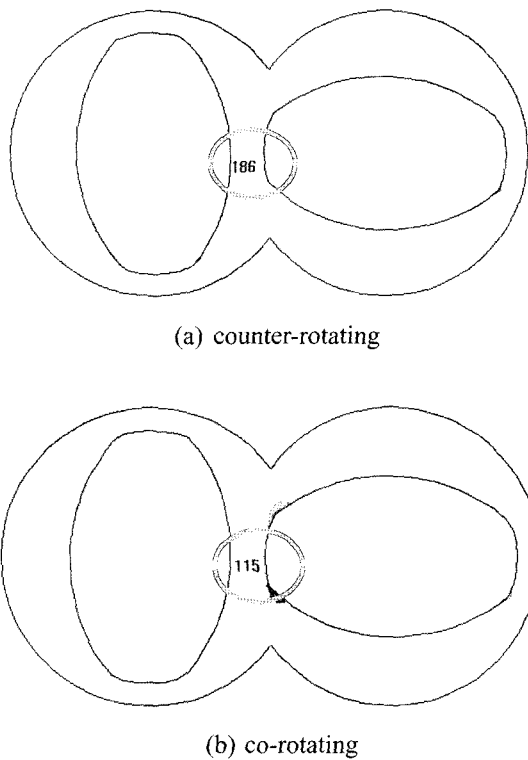


Fig. 17. Pressure distribution [kPa] in the cross section.

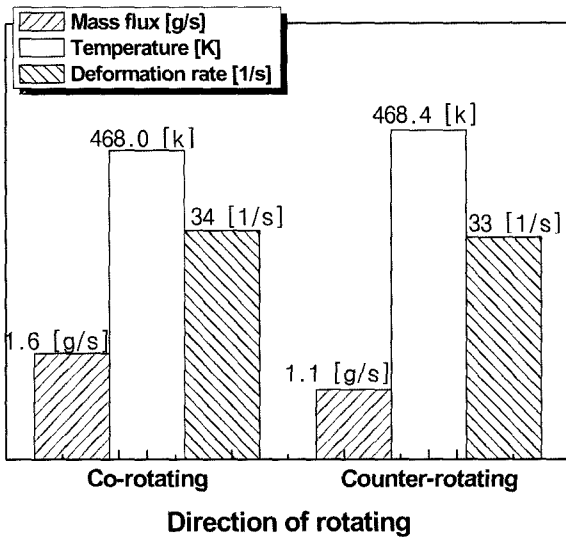


Fig. 18. Mass flux, temperature and shear rate with respect to the rotating direction.

melt from one side barrel to the other side barrel. It is advantageous to the mixing.

Fig. 18 shows the shear deformation rate, the mass flux, and the average temperature at outlet. We can figure out that the mass flux of the co-rotating screw extruder is higher but temperature is lower than those of the counter-rotating screw extruder. High mass flux in the co-rotating

screw extruder resulted from the high velocity component w comparing with the counter-rotating screw extruder. The average temperature at outlet of the counter-rotating screw extruder is higher due to the longer residence time as shown in Fig. 18.

Even though there is no significant difference in the overall deformation rates, there are differences in the elongation and the shear rates between the two screw extruders, respectively. The elongation rate is higher at counter-rotating screw extruder but the shear rate is higher at the co-rotating screw extruder as shown in Fig. 19. The total strain indicating the distributive mixing performance is 144 in the counter-rotating screw extruder which is higher than that in the co-rotat-

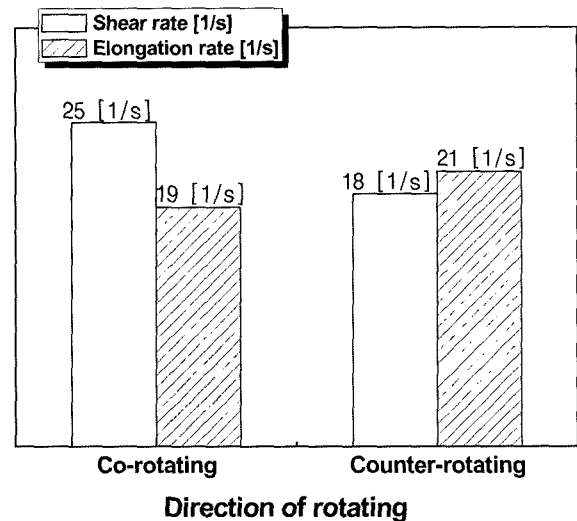


Fig. 19. Shear and elongation rate with respect to rotating direction.

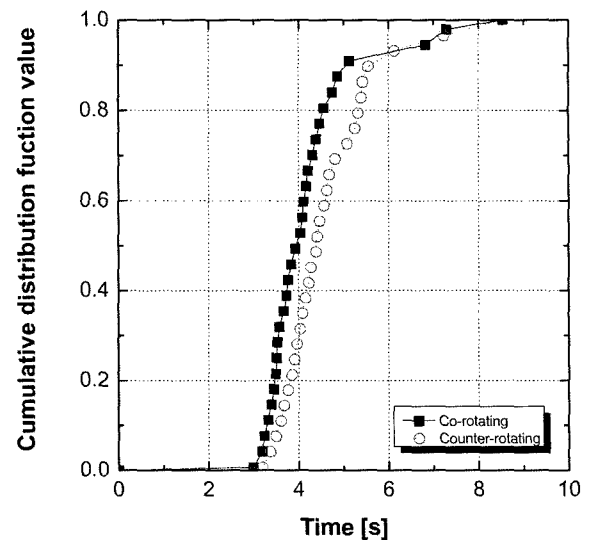


Fig. 20. Residence time distribution obtained from the numerical tracer experiment.

ing extruder (137). It is attributed to the longer residence time in the counter-rotating screw extruder as shown in Fig. 20. However, the co-rotating screw extruder is advantageous to the distributive mixing as described earlier.

5. Conclusions

We calculated the velocity field in the co-rotating screw element and analyzed the mixing performance with respect to the screw rotation speeds (60, 90, 120 rpm) and the pitch length (20, 40 mm) using a commercial code, STAR-CD. We also calculated the velocity field and the mixing performance in the counter-rotating screw extruder at 90 rpm and pitch size 30 mm and compared the mixing performance with that of the co-rotating screw extruder. From the results, we obtained the following conclusions.

1. The velocity components u and v are high near the screw surfaces and the velocity component w is high in the nip region where two screws cross over. It is resulted from the additive displacement effect due to the phase difference of two screws in the nip region.
2. The temperature is high near the screw surfaces and in the gap region where the deformation rate is high due to the heat generation by the viscous dissipation.
3. The pressure is high in front of the gap region in the rotational direction than that in back of the gap region. It is resulted from the decrease of available space for the flow of polymer melt.
4. As the screw rotation speed increases, the mass flux and the deformation rate increase but the residence time of polymer melt decreases. The rise of screw rotation speed results in the increase of the dispersive mixing performance.
5. When the screw pitch length is small, the mass flux decreases but the deformation rate and the residence time increase. It enhances the distributive mixing performance.
6. The conveying capacity and the distributive mixing performance of the co-rotating screw extruder are better than those of the counter-rotating screw extruder because the velocity component w in the co-rotating screw extruder is higher and the flow pattern is advantageous to the distributive mixing.

Acknowledgments

This work was financially supported by Agency for Defense Development.

References

- Bakalis, S. and M.V. Karwe, 2002, Velocity distributions and volume flow rates in the nip and translational regions of a co-rotating, self-wiping, twin-screw extruder, *Journal of Food Engineering* **51**, 273-282.
- Bravo, V.L. and A.N. Hrymak, 2000, Numerical simulation of pressure and velocity profiles in kneading elements of a co-rotating twin screw extruder, *Polymer Engineering and Science* **40**, 525-541.
- Bravo, V.L., A.N. Hrymak and J.D. Wricht, 2004, Study of particle trajectories, residence times and flow behavior in kneading discs of intermeshing Co-rotating twin-screw extruders, *Polymer Engineering and Science* **44**, 779-793.
- Cheng, H. and I.M. Zloczower, 1998, Distributive mixing in conveying elements of z ZSK-53 Co-rotating twin screw extruder, *Polymer Engineering and Science* **38**, 926-935.
- Ishikawa, T., S.I. Kihara and K. Funatsu, 2000, 3-D numerical simulations of nonisothermal flow in Co-rotating twin screw extruders, *Polymer Engineering and Science* **40**, 357-364.
- Ishikawa, T. and T. Amano, 2002, Flow pattern and mixing mechanisms in the screw mixing element of a Co-rotating twin-screw extruder, *Polymer Engineering and Science* **42**, 925-939.
- Jaluria, Y., M.V. Karwe and V. Sernas, 1996, Transport in a twin-screw extruder for the processing of polymers, *Polymer Engineering and Science* **36**, 1531-1540.
- Kajiwara, T., Y. Nagashima, Y. Nakano and K. Funatsu, 1996, Numerical study of twin-screw extruder by three-dimensional flow analysis-development of analysis technique and evaluation of mixing performance for full flight screws, *Polymer Engineering and Science* **36**, 2142-2152.
- Kim, N., H.B. Kim and J.W. Lee, 2006, Numerical analysis of internal flow and mixing performance in polymer extruder I: single screw extruder, *to be published*.
- Linjie, Z., A.N. Kwabena and S.H. Kun, 2005, Investigation of mixing mechanisms and energy balance in reactive extrusion using three-dimensional numerical simulation method, *International Journal of Heat and Mass Transfer* **48**, 3411-3422.
- Shearer, G. and C. Tzoganakis, 2000, The effects of kneading block design and operating conditions of distributive mixing in twin screw extruders, *Polymer Engineering and Science* **40**, 1095-1106.
- Ye, Y.S., H.B. Kim, N. Kim and J.W. Lee, 2005, A study on analysis of polymer extruder process using finite element method, *The Korean Society of Mechanical Engineers, Part A* **29**, 145-155.
- Yoshinaga, M., S. Katsuki, M. Miyazaki, L. Liu, S.I. Kihara and K. Funatsu, 2000, Mixing mechanism of three-tip kneading block in twin screw extruders, *Polymer Engineering and Science* **40**, 168-178.